This is an open access article published under an ACS AuthorChoice License, which permits copying and redistribution of the article or any adaptations for non-commercial purposes.

ACS OMEGA

http://pubs.acs.org/journal/acsodf

Mini-Review

Fabrication of Plasmonic Supercrystals and Their SERS Enhancing Properties

Maria Blanco-Formoso, Nicolas Pazos-Perez,* and Ramon A. Alvarez-Puebla*

Cite This: *ACS Omega* 2020, 5, 25485−25492

Read Online

ACCESS | Metrics & More | Article Recommendations

ABSTRACT: Supercrystals, made of ordered plasmonic nanoparticles (NPs) in close contact, turn out as efficient SERS substrates. However, the production of highly homogeneous structures implies precise control over a multitude of parameters including quality of the building blocks, solvent evaporation rate, and surface chemistry interactions. To pursue this goal, different approaches using templates to self-assembly NPs have been developed in recent years. Here, we review the most common procedures employing two different substrates, planar and patterned templates. Several approaches and strategies are described showing the optical properties of the resulted supercrystals and their behavior as SERS substrates.

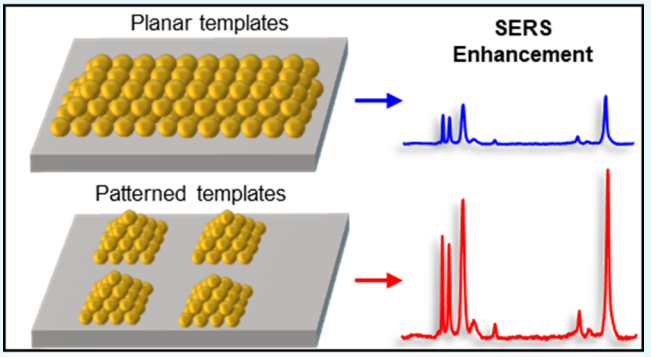

INTRODUCTION

The interest in the development of efficient surface-enhanced Raman scattering (SERS) substrates has been growing in recent years. The optical enhancing properties of individual NPs considerably improves when the particles are in close contact. Thus, the use of NPs as building blocks to fabricate highly ordered close-packed assemblies, known as colloidal crystals or supercrystals, has attracted the focus of interest of many research groups. Besides the individual inherent behavior of metallic NPs at the nanoscale, novel collective properties also emerge from these large organized materials at the macroscale. Regarding their use as SERS platforms, apart from the enhanced optical efficiency achieved by these architectures, the homogeneity in intensity along the crystals is crucial to obtain uniform and reproducible SERS signal for quantitative measurements. However, the achievement of efficient and homogeneous structures is not trivial, since a wide range of NP interactions (Coulombic, van der Waals, charge−dipole, dipole−dipole, entropic, capillary, convective, or shear), which guide the assembly process, are involved between the NPs, and with the substrate.[1] Further, external parameters like temperature, solvent polarity, or evaporation rate also play a key role. The successful formation of homogeneous supercrystals takes place only if the attractive forces between the NPs are large enough to overcome the entropy loss due to ordering.

Many different strategies have been developed during the past years in pursuit of the goal of homogeneous interactions between nanoparticles,[2] for instance, the assembly of colloidal NPs in solution or the use of colloidal templates to aggregate NPs at their surface.[3] Remarkably, the organization of NPs in macroscopic templates, allowing the formation of extended areas with highly ordered close-packed assemblies, give rise to easy manipulation, clean surfaces for direct SERS in solid, liquid, and gas phases.[4] Besides, it also allows the detection of analytes with low affinity to the plasmonic surfaces by simply casting them on the active templates or by functionalization of the material supercrystals with the appropriate selective molecules. In this regard, another approximation to create similar structures is the physical evaporation of metals on substrates.[5] Notwithstanding, the produced structures consist of heterogeneous polycrystalline islands with even gaps, thus providing heterogeneous field enhancement from point to point within the same sample. Thereby, bottom-up approaches based on nanoparticle self-assembly remains as one of the most useful alternatives. The production of large areas made of ordered NPs is achieved by inducing a convective flow of the NPs through the controlled evaporation of the solvent or the use of gravitational forces. In addition, structured crystals can be also formed using morphologically modified templates,[6] which are mostly fabricated by lithographic methods.

In this review, we focus on the different strategies proposed, to the present date, to produce homogeneous substrates made

Received: July 16, 2020
Accepted: September 15, 2020
Published: September 30, 2020

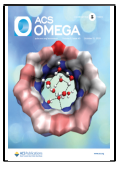

Downloaded via 88.14.36.24 on July 2, 2021 at 11:04:24 (UTC).
See https://pubs.acs.org/sharingguidelines for options on how to legitimately share published articles.

© 2020 American Chemical Society

https://dx.doi.org/10.1021/acsomega.0c03412
ACS Omega 2020, 5, 25485−25492

of plasmonic NPs organized at the surface of different templates, also showing their optical properties and their applicability in SERS sensing.

SPONTANEOUS ASSEMBLIES ON PLANAR TEMPLATES

The most common way to produce supercrystals on substrates is by the slow and controlled evaporation of highly concentrated colloidal solutions. This process generates a convective flow of the NPs inside the drop (Figure 1A).[7] The

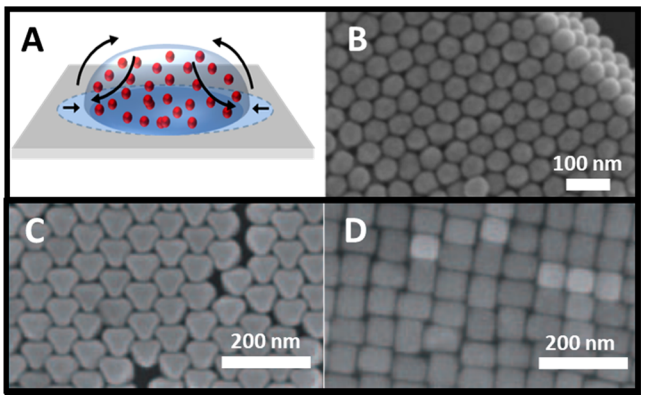

Figure 1. (A) Schematic representation of the convective flow assembly process. Representative scanning electron microscope (SEM) images of supercrystals formed with CTAB stabilized Au NPs of different morphologies: (B) spheres, (C) octahedra, and (D) cubes. (B) Adapted with permission from ref 25. Copyright 2011 American Chemical Society. (C,D) Adapted with permission from ref 16. Copyright 2011 John Wiley & Sons Ltd.

flow transports the particles from the drop edges to the bulk solution. This induces a nematic liquid crystalline phase above a critical NP concentration due to solvent evaporation leading to their organized sedimentation.[8] An alternative approach relies on the suppression of the evaporation of the solvent allowing slow gravitational sedimentation of the NPs on the template surface. This process is followed by the slow solvent evaporation as in the previous case.[9] By comparing both approaches, gradual sedimentation appears to provide a gentler driving force than solvent evaporation. Therefore, inducing more homogeneous large-scale assemblies. However, sedimentation requires the use of particles large enough to sediment with time. To form a crystal with the appropriate quality, the interplaying forces need to be considered. Thus, the organization of the particles within the crystal will depend on the following: (i) the quality of the building blocks; (ii) the solvent polarity; (iii) evaporation rate; (iv) substrate surface chemistry; and (v) surface chemistry of the NPs. It is clear that to achieve a homogeneous structure, the initial particles should be as homogeneous in size and shape as possible, with the threshold being a polydispersity below 10%.[7] Regarding the solvents, supercrystals can be produced in either polar or nonpolar solvents. Although nonpolar solvents induce better packing,[10] the restricted small NP size obtained during this type of synthesis produce less efficient hotspots and, thus, are not very common in SERS applications. In fact, the most popular methods for the fabrication of colloidal crystals usually employ water or water-miscible solvents. The evaporation rate is also a very important parameter. To induce the effective convective flow, which generates a vortex within the fluid for NP circulation, solvent evaporation must be slow. Thus, with slow evaporation, the thermocapillary Marangoni flow due to the temperature gradient between the droplet surface and the bulk is significantly increased. The substrate surface chemistry is also an important parameter to consider. For instance, the substrate charge should not be repulsive to the NPs. Additionally, the substrate wetting properties should be favorable to the solvent in order to achieve the proper contact angle between the NP drop and the substrate. Therefore, it is important to use hydrophilic substrates for aqueous base NPs solutions. Besides all these parameters, since the synthetic routes to produce NPs imply the use of surfactants, the NP surface chemistry is of special relevance. This fact is also directly related to the solvent surface tension and substrate wettability due to the presence of free surfactant molecules in solution. Therefore, NP solutions should be carefully cleaned from the excess of surfactants to avoid unwanted effects, such as the increase in hydrophobicity or substrate coating with charged surfactant molecules that may induce repulsions with the substrate. In addition, after solvent drying, the free surfactant in solution will form a compact thin film onto the crystal surface, thus hindering the interaction between the analyte molecules and the plasmonic surface. Therefore, plasma cleaning of the supercrystal once prepared is generally required.

The interaction between molecules at the surface of adjacent NPs is of relevant importance. In this regard, different surfactants behave differently. For instance, cetyltrimethylammonium bromide (CTAB), which is the most used surfactant for the synthesis of plasmonic NPs, induces a close packing assembly of the NPs. This effect is ascribed to the bilayer of CTAB formed around the NPs. Thus, when the NPs became closer to each other while drying, interdigitation of CTAB molecules between neighboring NPs occurs, inducing their assembly already in solution.[11] Therefore, CTAB concentration in the NP solutions should be as low as possible but still high enough to stabilize the colloids. This assembly approach is effective independently of the morphology of the NPs. However, the building block morphology strongly influences the final packing lattice of the supercrystal. For instance, spheres or octahedra assemble in hexagonal lattices, meanwhile cubes organize in a square lattice (Figure 1B–D).[12−16]

Optical properties and SERS efficiency of these structures are both strongly dependent on the NP size and shape. The interparticle gap distances between CTAB stabilized NPs have been reported to be around 3–5 nm.[15,17] Therefore, a strong plasmonic coupling between the NPs is generated exhibiting an electric field accumulation on the top layer of the superlattice.[15,17] This can be clearly observed in Figure 2A for the case of spherical NPs by comparing the UV–vis-NIR spectra of Au NPs of different sizes either in solution or by forming supercrystals. The SERS performance of these crystals was also studied based on the NP size using benzenethiol (BT) in the gas phase (Figure 2B). Notably, the optical enhancing ability of the superlattices increases with the size of nanoparticles to a maximum of 214 nm, and then, the intensity abruptly decreases with size (Figure 2C). Selected SERS intensity maps of these structures (Figure 2D) demonstrate the SERS intensity uniformity within the samples.[15]

The assembly of anisotropic NPs introduces extra complexity in the structures. For instance, when nanorods (NRs) are used to produce supercrystals, they can self-organize into close-packed layers either parallel or vertically aligned (Figure

https://dx.doi.org/10.1021/acsomega.0c03412
ACS Omega 2020, 5, 25485−25492

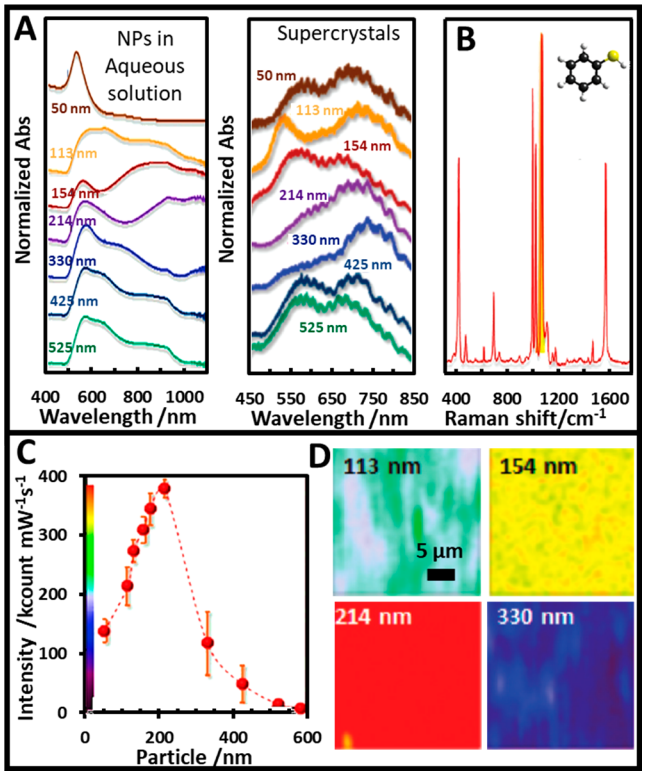

Figure 2. (A) Experimental UV−vis-NIR spectra of spherical Au NPs of different sizes, from 50 to 885 nm, in solution and forming supercrystals. (B) SERS spectra of BT obtained from a supercrystal. (C) SERS intensity of the crystals as a function of the NP size. (D) SERS intensity maps (21 × 21 μm^2) from four selected NPs sizes supercrystals. (λ_{ex}: 785 nm) Adapted with permission from ref 15. Copyright 2012 American Chemical Society.

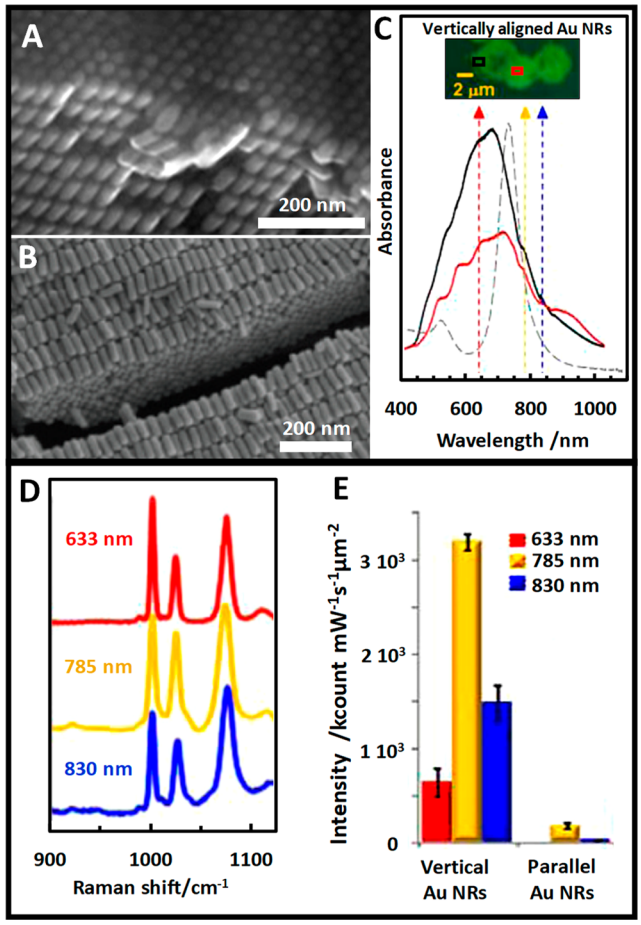

Figure 3. (A,B) Representative SEM images of supercrystals formed from organized Au nanorods oriented either (A) vertically or (B) parallel to the substrate. (C) Optical image of a vertically assembled NRs supercrystal and the corresponding dark-field localized surface plasmon resonance bands at the edges (black) and at the center (red) together with the spectra of the individual NRs in solution (gray). Dotted arrows indicate the excitation laser lines used for SERS. (D) Representative SERS spectra of benzenethiol and (E) its corresponding SERS intensities at 1072 cm^{-1} for the two different crystal configurations and for three different laser lines as compared with nanorods in solution. (A,C,D,E) Adapted with permission from ref 17. Copyright 2011 National Academy of Sciences USA. (B) Adapted with permission from ref 18. Copyright 2012 American Chemical Society.

3A,B)[18] generating, in both cases, surfaces with active hot spots. Note that the surface plasmon resonance becomes complex as compared with that of the initial rods in solution (Figure 3C). SERS detection limits for parallel (side-to-side) configuration have been reported to produce lower enhancement factors than vertical (tip-to-tip) assemblies due to the field localization at the NR tips (Figure 3D, E). In the same way, Au NRs coated with Ag have been also used to produce similar assemblies, exhibiting around 2.5-fold higher enhancement than AuNRs. In this case, the vertically aligned crystals also give rise to larger intensities (4-fold when excited with a 633 nm laser line) than the parallel structures.

The driving forces inducing the NRs to selective assembly parallel or vertically to the substrates are not completely understood. However, it has been reported that higher NRs concentration promotes standing up configuration.[19] In addition, other surfactants like (11-mercaptoundecyl)hexa-(ethylene glycol) (MUDOL) or the cationic gemini surfactant (oligooxa)alkanediyla, w-bis(dimethyldodecylammonium bromide) have been reported to favor the formation of vertically aligned NRs through chains' interdigitation.

The fabrication of supercrystals of silver nanoparticles is more restricted in terms of size and shape. However, using the polyol method, different particle morphologies, including cubes, truncated cubes, cuboctahedra, truncated octahedra and octahedra, have been produced. This approach requires the use of dimethylformamide (DMF) and polyvinylpyrrolidone (PVP) as stabilizer.[9] Here, the NPs are coated with a thick layer of polymer. When the polymer layers of two NPs come into contact, the strong van der Waals attraction results in a polymer restructuration with a reported interparticle gap of approximately 6 nm.[20] Figure 4 shows supercrystals made of Ag NPs with different packing lattices depending on the building blocks' morphology. Regarding their use as SERS platforms, EFs of these types of crystals have been reported to be around 10^6. It is worth noting that crystals made of silver are susceptible to oxidation, and thus, conventional oxygen plasma cleaning cannot be applied.

Finally, an intrinsic issue of the droplet evaporation process in the supercrystal formation is the well-known coffee-ring effect which disturbs its homogeneous formation when drying. This issue has been addressed by modifying the wetting properties between the solution and the substrate using, for instance, MUDOL to stabilize the NPs. In fact, this surfactant decreases the contact angle between the drop and the

https://dx.doi.org/10.1021/acsomega.0c03412
ACS Omega 2020, 5, 25485−25492

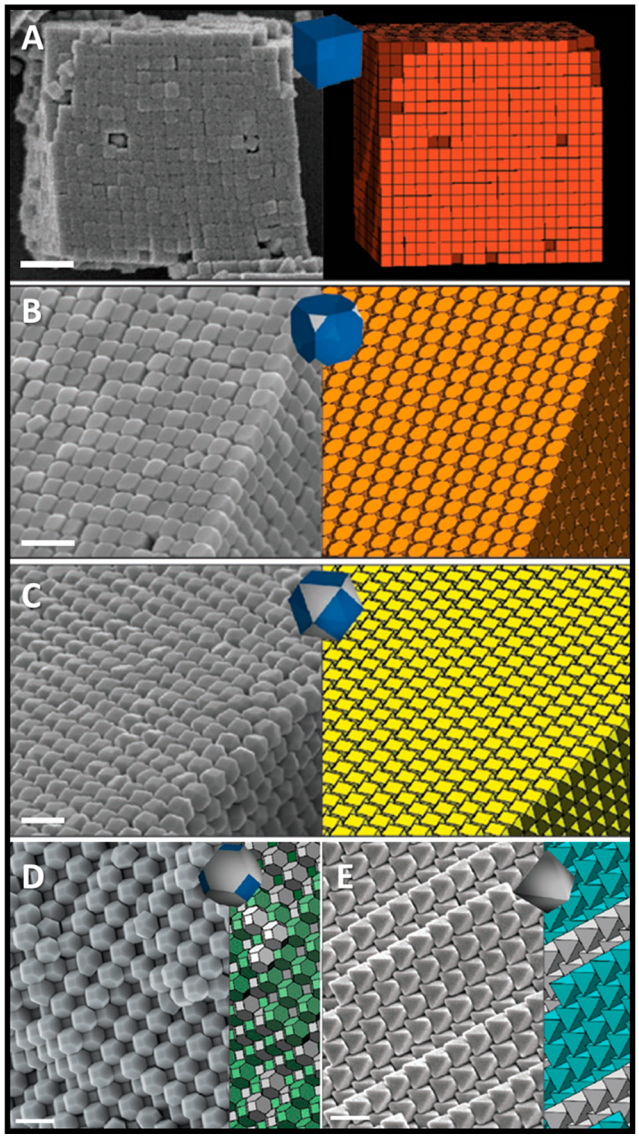

Figure 4. Representative SEM images and their corresponding lattice packing diagrams of supercrystals formed with different Ag NP shapes: (A) cubes, (B) truncated cubes, (C) cuboctahedra, (D) truncated octahedra, and (E) octahedra. Colors in D and E indicate different layers of the crystal that do not lie in the same plane. Scale bars are 500 nm. Adapted with permission from ref 14. Copyright 2012 Macmillan Publishers Limited.

substrate. Therefore, due to a smaller contact between them, a smaller and thicker concentrated crystal is formed suppressing the coffee-ring effect.

IMPRINTED ASSEMBLIES WITH PATTERNED MASTERS

The production of structured arrays of NPs has also been addressed by similar approaches as for planar templates, with the most common ones being the convective controlled evaporation and gravitational sedimentation. The main difference is that to achieve structured assemblies, templates with concrete topographic features are required. In this regard, the most common way to produce these templates is by lithographic methods. For example, Au NP dimers were fabricated using a lithographic pattern silicon wafer with periodically arrange nanoholes of 120 nm in diameter. The process consists of dip coating the substrate in an aqueous NPs solution under controlled evaporation. During this evaporation, the meniscus moves back concentrating the particles in the three-phase contact point (template, air, solvent) and capillary forces coerce the particles to enter into the holes. The SERS enhancement factor of these assemblies was reported to be 10^9 when using benzenethiol as reporter and incident light polarization parallel to the dimer axis (Figure 5A).[21] In a

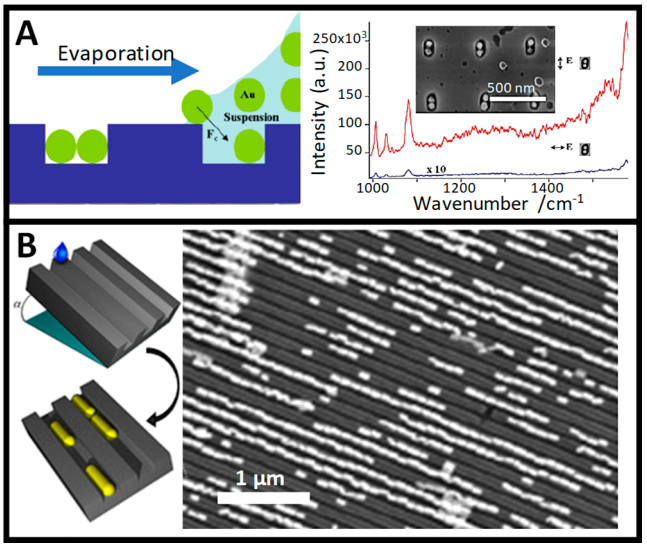

Figure 5. (A) Fabrication of a periodic array of Au NP dimers produced when capillary forces coerce the NPs to enter the holes of a template as the meniscus moves back when drying. SEM image (inset) and SERS spectra benzenethiol adsorbed onto single gold dimer where incident light is parallel (red) and perpendicular (blue) to the dimer axis. (B) Assembly approach where a patterned template with nanochannels is positioned at an angle to promote the NP flow from a droplet cast to the nanochannels. SEM image of linear arrays of Au NRs produced by this approach. (A) Adapted with permission from ref 21. Copyright 2009 John Wiley & Sons Ltd. (B) Adapted with permission from ref 22. Copyright 2017 American Chemical Society.

similar fashion, lines of Au NPs were produced by using a silica substrate with nanochannels where a drop of NPs was placed between the lithographic template and a glass substrate. During the drying process, the aqueous surface line moves backward, inducing the assembly of the NPs into the channels. Depending on the width of the channels, lines composed of different NPs (single, double, or more) can be produced. This approach has also been modified by controlling the motion of the template using a motorized translation stage to physically recede the contact line between the template and the glass slide parallel to the channels. As for nonspherical NPs, 1D ordered structures of gold nanorods have also been produced using a patterned silicon template with nanochannels. In this case, the template was inclined and covered with a glass slide, to further cast the NRs solution onto the elevated edge. Due to capillarity, the solution flows down through the channels inducing a chain-like alignment of the NRs during the evaporation process (Figure 5B).[22]

Although lithographic methods have been proven to be an effective way to produce morphological directed assemblies of NPs, these protocols present several drawbacks related to their complex manufacturing with an elevated production cost and the brittleness of the templates. Therefore, to avoid the use of

https://dx.doi.org/10.1021/acsomega.0c03412
ACS Omega 2020, 5, 25485−25492

these expensive platforms, different alternatives have been proposed. Among all of them, the most popular is the use of elastomers like polydimethylsiloxane (PDMS) to replicate the morphological features of lithographic templates. This process, known as replica molding, has the advantages of providing flexibility, reusability, and tunable hydrophobicity to the templates. Therefore, they are easy to handle; meanwhile, their production is also easier and cheaper. In addition, the use of PDMS as a template allows the selective hydrophilization of concrete areas through O_2 plasma oxidation in order to confine the NPs drop. Using this approach, NPs can sediment in a humidity chamber to avoid solvent evaporation and autoassemble during sedimentation driven by capillary and gravitational forces. After solvent drying, the satisfactory structured organization of the supercrystals can be easily transferred to any surface employing adhesive double tape.[23] For example, 3D pyramidal crystals arrays were fabricated using Au nanospheres as building blocks. They were produced either via convective flow (confining the NPs between the structured PDMS and a glass slide)[24] or by confinement gravitational sedimentation[6] (Figure 6A,B). The main difference between both approaches is that the first one produces discrete pyramids on the template while the second approach gives rise to pyramids connected underneath with a continuous crystal. Detection of CV up to 10^{-12} M was shown (Figure 6C) ascribed to a significant signal concentration at the pyramid tip (Figure 6D) due to the antenna effect, in a similar way as for other supercrystals. This effect was confirmed by high-resolution confocal SERS measurements on a single pyramid with a spatial resolution of 500 nm (Figure 6E).[6] Besides, the second approach (gravitational sedimentation) can also be used to create discrete supercrystals. To do that, after NP sedimentation, instead of letting the drop evaporate, a cleaning step using spin coating with water can be applied to remove the excess NPs from the template surface (Figure 6F).[23] Figure 6G shows different supercrystal morphologies obtained with this methodology such as cubes (i), toroids (ii), or cubes connected among them (iii).[23]

The SERS enhancing properties of crystals with different morphological features were tested and compared by depositing a monolayer of BT in the gas phase using a near-infrared (785 nm) laser. For this comparison, the height of the crystals was maintained constant, while the side dimensions for different morphologies were varied. A regular continuous nanoparticle film was also analyzed for comparison. The SERS intensity for crystals with different sizes and morphologies is shown in Figure 6H. After observing those results, two main conclusions can be stated. The first one is that topographic patterned crystals provide a consistently larger SERS intensity than flat continuous crystals. The second observation is that the SERS intensity is similar independent of the crystal geometry, which is directly related to the crystals' side dimensions, becoming more intense for larger crystals.[23] This strategy has been commonly used to regularly organize NPs in 2D and 3D arrays.[24]

Although replica molding is an easy and low-cost method to produce morphological templates, it still requires the use of generally lithographic substrates to use as molds, considerably restricting their applicability. Therefore, different approaches to avoid the use of lithographic templates have been studied. One proposed alternative to lithographic templates is the anodization of an aluminum template to produce a periodic linear parallel array nanostructure. Due to the narrow width of

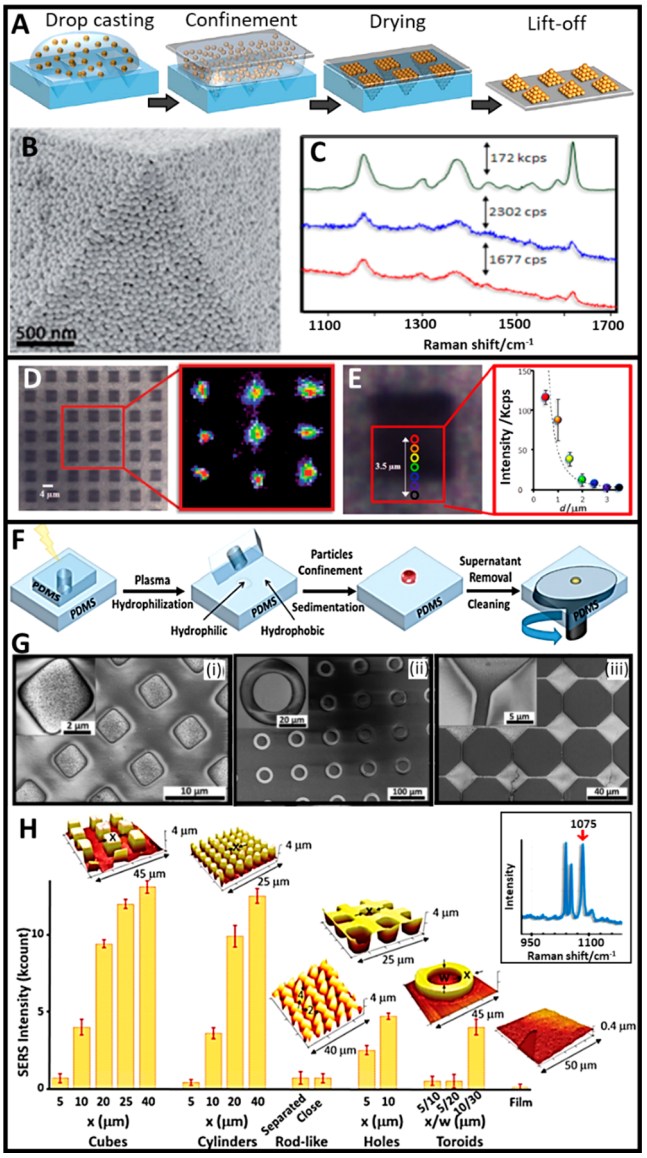

Figure 6. (A) Fabrication of nanopyramids composed of gold spheres. (B) High-resolution SEM images of a pyramidal supercrystal (side length of 4.4 μm and a height of 3.0 μm). (C) SERS detection of crystal violet (CV) on the pyramids. Green spectrum represents the resembled SERS signal of CV; meanwhile, blue and red spectra are the corresponding signals obtained at two different spots of the array using a minute amount of CV (0.06 molecules/μm^2). (D) Optical image and SERS mapping of the ring stretching band of 1-naphthalenethiol (1368 cm^{-1}), showing how higher intensities are localized at the top of the pyramids. (E) Optical image of one pyramidal structure and SERS intensities provided by different areas of the structure. (F) Fabrication of supercrystals arrays with multiple geometries. (G) SEM images of supercrystals with different morphologies. (H) Comparison of the SERS intensities for different supercrystal morphologies as a function of the crystals width. (A) Adapted with permission from ref 24. Copyright 2017 American Chemical Society. (B–E) Adapted with permission from ref 6. Copyright 2013 John Wiley & Sons Ltd. (F–H) Adapted with permission from ref 23. Copyright 2016 The Royal Society of Chemistry.

the produced grooves (36 nm), this template forces the organization of NRs into tip-to-tip configuration via spin-coating. The as-produced NRs assembly presents an inherent hydrophobicity. Therefore, aqueous phase analytes concentrate

https://dx.doi.org/10.1021/acsomega.0c03412
ACS Omega 2020, 5, 25485−25492

on a small spatial region of the substrate resulting in an improvement of the SERS efficiency. Comparison between these substrates and commercial Klarite results in a 40-fold higher SERS intensity when using 2-naphthoic acid in aqueous phase.[6]

Another interesting alternative to lithographic templates is the production of wrinkled templates. This approach consists of the use of elastomeric materials like PDMS that are submitted to a single-axial strain while the surface is oxidized producing a harder layer on top. After releasing the strength, periodic linear arrays are produced. Using this approach, NPs can be assembled into the grooves in a similar fashion as explained before, the most common way being the direct stamping of a drop of NPs with the structured PDMS on a substrate[25] or by spin coating the NPs on the PDMS template. In addition, by modifying the wrinkle wavelength and the NPs size, single, double, or more densely packed line assemblies can be obtained. The use of PDMS substrates for direct assembly has the advantage of allowing the transfer of the NP arrays to a target substrate by the stamping approach using a water droplet after the assembly. Parallel lines of single and double 66 nm Au nanospheres were tested as uniform and efficient SERS substrates.[25] Figure 7A shows the schematic representation of the stamping process and the corresponding SEM images of the assembled NPs. Figure 7B shows the white light, dark field, and SERS images (normalized at 1072 cm^{-1}) obtained for single and double line arrays after testing benzenethiol as the molecular probe. The average SERS intensity shown in Figure 7B shows a slightly higher intensity for double lines; however, when calculating the SERS intensity per particle, it shows that the ordering into single NP lines is more efficient than for double lines, with 155 counts for the single line and 99 counts for the double line. The wrinkle template method has also been applied to organize NRs and stars in lines. Interestingly, by applying strain forces in different axes to the elastomeric material, other patterns based on linear interferences can be achieved. Nevertheless, although the wrinkling method is very simple and low cost, its morphological versatility is very limited. Therefore, to produce periodic complex geometries, the use of PDMS for replica molding is still required.

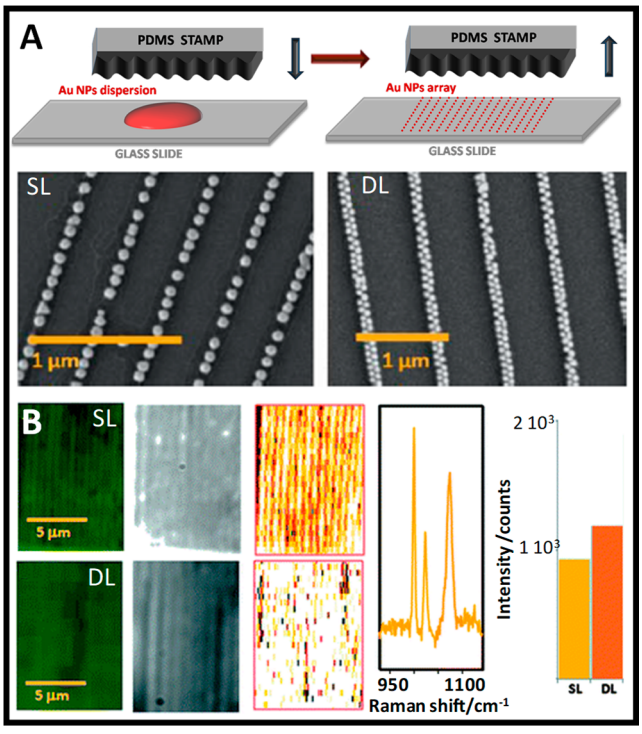

Figure 7. (A) Fabrication of parallel arrays of Au NPs through the stamping of a PDMS wrinkle template and the corresponding SEM images of single (left) and double (right) lines. (B) Optical, dark field, and SERS images of single (up) and double (down) lines, together with the representative SERS spectrum of BT and the comparison of the corresponding SERS intensities at 1072 cm^{-1} between single and double lines. (A,B) Adapted with permission from ref 25. Copyright 2010 The Royal Society of Chemistry.

CONCLUSIONS AND OUTLOOK

In summary, significant advances have been achieved to produce template supported supercrystals. In this regard, different parameters like the surfactants used or solvent evaporation features considerably influence the homogeneity and precise control over the resulted structures. The most successful approach is the use of cationic amphiphilic surfactants like CTAB or MUDOL together with a controlled low evaporation rate of the solvent. Among the different strategies to construct patterned templates, replica molding is presented as a more suitable procedure in comparison with lithographic methods. Even if both give rise to a multitude of continuous and discrete supercrystals of different shapes and sizes, replication allows an easy-handling and low-cost production. Regarding the SERS enhancing properties, patterned crystals result in a better SERS performance versus planar structures.

Despite the great advances achieved, further understanding of the forces which guide the NP self-assembly is required in order to refine the fabrication of the desired supercrystals. In addition, to boost the SERS optical activity of the crystals, better control over the synthesis of Ag NPs with protocols to protect them against oxidation will be desired. Moreover, easy procedures as an alternative to replica molding (which still requires the initial use of lithographic templates) that allow a cheap and mass production of patterned templates are still required.

AUTHOR INFORMATION

Corresponding Authors

Nicolas Pazos-Perez − *Department of Physical Chemistry, Universitat Rovira i Virgili, 43007 Tarragona, Spain;* orcid.org/0000-0002-2326-4231; Email: nicolas.pazos@urv.cat

Ramon A. Alvarez-Puebla − *Department of Physical Chemistry, Universitat Rovira i Virgili, 43007 Tarragona, Spain; ICREA, 08010 Barcelona, Spain;* orcid.org/0000-0003-4770-5756; Email: ramon.alvarez@urv.cat

Author

Maria Blanco-Formoso − *Department of Physical Chemistry, Universitat Rovira i Virgili, 43007 Tarragona, Spain*

Complete contact information is available at: https://pubs.acs.org/10.1021/acsomega.0c03412

Notes

The authors declare no competing financial interest.

https://dx.doi.org/10.1021/acsomega.0c03412
ACS Omega 2020, 5, 25485−25492

Biographies

Dr. Maria Blanco-Formoso focuses her research on the development of plasmonic nanostructures which can act as SERS sensors for different diseases. She has a Ph.D. from the University of Vigo (2019) and currently is a postdoctoral researcher in the Plasmonics and Ultradetection Zeptonic group (Department of Physical and Inorganic Chemistry) at the University Rovira i Virgili (Tarragona, Spain).

Dr. Nicolas Pazos-Perez is a specialist in colloidal chemistry focused on the synthesis and surface functionalization of plasmonic nanoparticles and their self-assembly into ordered structures. Currently, his work involves the use of these materials as SERS-based detection systems. He has a degree in chemistry (Universidade de Vigo, 2004) and performed his doctoral studies (2008) within the frame of Marie Curie Research Training Network between Spain and Germany at the Universidade de Vigo and the Center of Advanced Studies and Research in Bonn. After this period, he joined the University of Bayreuth (Germany) as a Postdoctoral Research Associate. In 2013 he moved back to Spain (Tarragona), and became a Senior Researcher officer at Medcom Advance. In 2014 he was awarded with a Marie Curie Fellow and joined the Plasmonics and Ultradetection Group (Zeptonic) at the University Rovira i Virgili (Tarragona, Spain) where he continues within the Ramon y Cajal program.

Prof. Ramon A. Alvarez-Puebla is an expert in surface science, nanoscience, and spectroscopy with emphasis on the manufacture and characterization of plasmonic materials and their integration into advanced detection devices especially with application in nanobiomedicine. He has a degree in chemistry (Universidad de Navarra, 2000) and a doctorate in surface science (Universidad Publica de Navarra, 2003, summa cum laude). He completed his postdoctorate at the University of Windsor (Windsor, ON, Canada) and General Motors Corporation (Warren, Mi, USA) in nanofabrication and surface spectroscopy (SERS, SEFS, and SEIRA) with Prof. Ricardo Aroca (UWINDSOR) and the Prof. Gholam Abbas Nazri (GMC). During 2006−2007, he worked as Research Officer and Principal Investigator at the National Institute for Nanotechnology of the National Research Council of Canada (NINT-NRC, Edmonton, AB, Canada). In 2008, he returned to Spain as associate Professor at the Universidade de Vigo. Since 2012 he has been ICREA Professor at the Universitat Rovira i Virgili in Tarragona, where he leads the Plasmonics and Ultradetection Group (Zeptonic).

■ ACKNOWLEDGMENTS

Authors acknowledge the Spanish Ministerio de Economia y Competitividad (CTQ2017-88648R and RYC-2015-19107), the Generalitat de Cataluña (2017SGR883) and the Universitat Rovira I Virgili (FR 2019-B2).

■ REFERENCES

(1) Silvera Batista, C. A.; Larson, R. G.; Kotov, N. A. Nonadditivity of nanoparticle interactions. *Science* **2015**, *350* (6257), 1242477.

(2) Kotov, N. A.; Meldrum, F. C.; Wu, C.; Fendler, J. H. Monoparticulate Layer and Langmuir-Blodgett-Type Multiparticulate Layers of Size-Quantized Cadmium Sulfide Clusters: A Colloid-Chemical Approach to Superlattice Construction. *J. Phys. Chem.* **1994**, *98* (11), 2735−2738.

(3) Blanco-Formoso, M.; Pazos-Perez, N.; Alvarez-Puebla, R. A. Fabrication and SERS properties of complex and organized nanoparticle plasmonic clusters stable in solution. *Nanoscale* **2020**, *12*, 14948−14956.

(4) Wang, R.; Yan, X.; Ge, B.; Zhou, J.; Wang, M.; Zhang, L.; Jiao, T. Facile Preparation of Self-Assembled Black Phosphorus-Dye Composite Films for Chemical Gas Sensors and Surface-Enhanced Raman Scattering Performances. *ACS Sustainable Chem. Eng.* **2020**, *8* (11), 4521−4536.

(5) Hicks, E. M.; Lyandres, O.; Hall, W. P.; Zou, S.; Glucksberg, M. R.; Van Duyne, R. P. Plasmonic Properties of Anchored Nanoparticles Fabricated by Reactive Ion Etching and Nanosphere Lithography. *J. Phys. Chem. C* **2007**, *111* (11), 4116−4124.

(6) Alba, M.; Pazos-Perez, N.; Vaz, B.; Formentin, P.; Tebbe, M.; Correa-Duarte, M. A.; Granero, P.; Ferre-Borrull, J.; Alvarez, R.; Pallares, J.; Fery, A.; de Lera, A. R.; Marsal, L. F.; Alvarez-Puebla, R. A. Macroscale plasmonic substrates for highly sensitive surface-enhanced Raman scattering. *Angew. Chem., Int. Ed.* **2013**, *52*, 6459−6463.

(7) Shevchenko, E. V.; Talapin, D. V.; Kotov, N. A.; O'Brien, S.; Murray, C. B. Structural diversity in binary nanoparticle superlattices. *Nature* **2006**, *439* (7072), 55−9.

(8) Guerrero-Martínez, A.; Pérez-Juste, J.; Carbó-Argibay, E.; Tardajos, G.; Liz-Marzán, L. M. Gemini-Surfactant-Directed Self-Assembly of Monodisperse Gold Nanorods into Standing Superlattices. *Angew. Chem., Int. Ed.* **2009**, *48* (50), 9484−9488.

(9) Tao, A.; Sinsermsuksakul, P.; Yang, P. Polyhedral silver nanocrystals with distinct scattering signatures. *Angew. Chem., Int. Ed.* **2006**, *45* (28), 4597−4601.

(10) Udayabhaskararao, T.; Altantzis, T.; Houben, L.; Coronado-Puchau, M.; Langer, J.; Popovitz-Biro, R.; Liz-Marzán, L. M.; Vuković, L.; Král, P.; Bals, S.; Klajn, R. Tunable porous nanoallotropes prepared by post-assembly etching of binary nanoparticle superlattices. *Science* **2017**, *358* (6362), 514.

(11) Sau, T. K.; Murphy, C. J. Self-Assembly Patterns Formed upon Solvent Evaporation of Aqueous Cetyltrimethylammonium Bromide-Coated Gold Nanoparticles of Various Shapes. *Langmuir* **2005**, *21* (7), 2923−2929.

(12) Huang, Y.; Kim, D.-H. Synthesis and Self-Assembly of Highly Monodispersed Quasispherical Gold Nanoparticles. *Langmuir* **2011**, *27* (22), 13861−13867.

(13) Lee, Y. H.; Lay, C. L.; Shi, W.; Lee, H. K.; Yang, Y.; Li, S.; Ling, X. Y. Creating two self-assembly micro-environments to achieve supercrystals with dual structures using polyhedral nanoparticles. *Nat. Commun.* **2018**, *9* (1), 1−8.

(14) Henzie, J.; Grünwald, M.; Widmer-Cooper, A.; Geissler, P. L.; Yang, P. Self-assembly of uniform polyhedral silver nanocrystals into densest packings and exotic superlattices. *Nat. Mater.* **2012**, *11* (2), 131−137.

(15) Pazos-Perez, N.; Garcia de Abajo, F. J.; Fery, A.; Alvarez-Puebla, R. A. From Nano to Micro: Synthesis and Optical Properties of Homogeneous Spheroidal Gold Particles and Their Superlattices. *Langmuir* **2012**, *28* (24), 8909−8914.

(16) Zhu, Z.; Meng, H.; Liu, W.; Liu, X.; Gong, J.; Qiu, X.; Jiang, L.; Wang, D.; Tang, Z. Superstructures and SERS Properties of Gold Nanocrystals with Different Shapes. *Angew. Chem., Int. Ed.* **2011**, *50* (7), 1593−1596.

(17) Alvarez-Puebla, R. A.; Agarwal, A.; Manna, P.; Khanal, B. P.; Aldeanueva-Potel, P.; Carbó-Argibay, E.; Pazos-Pérez, N.; Vigderman, L.; Zubarev, E. R.; Kotov, N. A.; Liz-Marzán, L. M. Gold nanorods 3D-supercrystals as surface enhanced Raman scattering spectroscopy substrates for the rapid detection of scrambled prions. *Proc. Natl. Acad. Sci. U. S. A.* **2011**, *108* (20), 8157.

(18) Ye, X.; Jin, L.; Caglayan, H.; Chen, J.; Xing, G.; Zheng, C.; Doan-Nguyen, V.; Kang, Y.; Engheta, N.; Kagan, C. R.; Murray, C. B. Improved Size-Tunable Synthesis of Monodisperse Gold Nanorods through the Use of Aromatic Additives. *ACS Nano* **2012**, *6* (3), 2804−2817.

(19) Tebbe, M.; Maennel, M.; Fery, A.; Pazos-Perez, N.; Alvarez-Puebla, R. A. Organized Solid Thin Films of Gold Nanorods with Different Sizes for Surface-Enhanced Raman Scattering Applications. *J. Phys. Chem. C* **2014**, *118* (48), 28095−28100.

(20) Tao, A. R.; Ceperley, D. P.; Sinsermsuksakul, P.; Neureuther, A. R.; Yang, P. Self-Organized Silver Nanoparticles for Three-Dimensional Plasmonic Crystals. *Nano Lett.* **2008**, *8* (11), 4033−4038.

https://dx.doi.org/10.1021/acsomega.0c03412
ACS Omega 2020, 5, 25485−25492

(21) Alexander, K. D.; Hampton, M. J.; Zhang, S.; Dhawan, A.; Xu, H.; Lopez, R. A high-throughput method for controlled hot-spot fabrication in SERS-active gold nanoparticle dimer arrays. *J. Raman Spectrosc.* **2009**, *40* (12), 2171−2175.
(22) Ashkar, R.; Hore, M. J. A.; Ye, X.; Natarajan, B.; Greybush, N. J.; Lam, T.; Kagan, C. R.; Murray, C. B. Rapid Large-Scale Assembly and Pattern Transfer of One-Dimensional Gold Nanorod Superstructures. *ACS Appl. Mater. Interfaces* **2017**, *9* (30), 25513−25521.
(23) Tebbe, M.; Lentz, S.; Guerrini, L.; Fery, A.; Alvarez-Puebla, R. A.; Pazos-Perez, N. Fabrication and optical enhancing properties of discrete supercrystals. *Nanoscale* **2016**, *8* (25), 12702−12709.
(24) Hanske, C.; González-Rubio, G.; Hamon, C.; Formentín, P.; Modin, E.; Chuvilin, A.; Guerrero-Martínez, A. s.; Marsal, L. F.; Liz-Marzán, L. M. Large-scale plasmonic pyramidal supercrystals via templated self-assembly of monodisperse gold nanospheres. *J. Phys. Chem. C* **2017**, *121* (20), 10899−10906.
(25) Pazos-Pérez, N.; Ni, W.; Schweikart, A.; Alvarez-Puebla, R. A.; Fery, A.; Liz-Marzán, L. M. Highly uniform SERS substrates formed by wrinkle-confined drying of gold colloids. *Chem. Sci.* **2010**, *1* (2), 174−178.

https://dx.doi.org/10.1021/acsomega.0c03412
ACS Omega 2020, 5, 25485−25492